# Sensitivity of Nickel Oxide Nanoflakes Layer on Extend Gate Field Effect Transistor for pH Sensor

**Dauda Abubakar, Naser M. Ahmed, and Zakariyya Uba Zango**

**Abstract** Nickel oxide (NiO) nanoflakes films for Extended gate field effect transistor (EGFET) pH sensors were synthesized and deposited by chemical bath deposition (CBD) method on indium titanium oxide (ITO) with glass substrate. The properties of NiO nanoflakes layer and pH sensing behaviour of the device were studied. Field emission scanning electron microscopy (FESEM) result shows that the $NiO/Ni(OH)_2$ films consists of porous net-like structure made up of interconnected nanoflake wall, with wall thickness of about 300 nm for the annealed NiO layer sample at 300 °C. XRD (X-ray diffraction) analysis demonstrated that the NiO nanoflakes has a cubic structure with the preferential orientation of the films at (100), (200) and (220). The devices exhibited superior sensing characteristic, due to the small size of the crystal and wide pore/flakes wall size of the NiO layer. The results confirmed that the NiO nanoflakes membrane has high sensitivity (72 µA/pH and 57 mV/pH) as compared with previews reports on NiO as sensing membrane for pH sensor.

**Keywords** Nickel oxide · Nanoflakes · pH sensor · EGFET · Chemical bath deposition

## 1 Introduction

The role Hydrogen ion concentration in the field of physical, biological and chemical sciences is important. A precise pH concentration measurement for a particular

D. Abubakar (✉)
Department of Physics, Bauchi State University Gadau, 65 Itas/Gadau, Bauchi, Nigeria

N. M. Ahmed
School of Physics, Universiti Sains Malaysia, 11800 Pulau Pinang, Malaysia
e-mail: naser@usm.my

Z. U. Zango
Department of Chemistry, College of Natural and Applied Sciences, Al-Qalam University, Katsina, Nigeria

system is needed in various experimental analysis for research and experimental applications. Glass electrodes have been used in the measurement of pH due to its higher sensitivity. But the high instability in corrosive solutions, high impedance of glass membrane and miniaturization difficulty fragility, limit the glass electrode application for pH sensor devices [1].

Therefore, to minimize the effect related to glass electrode, the Ion sensitive field effect transistor (ISFET) has been employed based metal oxide field effect transistor (MOSFET). However, as time goes on, the ISFET was observed to be facing some imperfection due to its highly instability in solution of saline water with sensitivity of light [2].

The Extended gate field effect transistor (EGFET) was advanced with the FET isolation structure from the metal oxide, that separates part of the chemical solution from the FET. EGFET structure is made of two separate parts; (1) commercial standard MOSFET and (2) sensing membrane cell. It comes along with so many advantages, which include easy maintenance, low cost, simple structure, free from chemical environment as well as light and temperature sensitivity. Nowadays, EGFETs has got great attention due to its vast advantages over others [3].

However, different metal oxides have been developed as the sensing membrane for EGFETs, such as $PtO_2$, ZnO [4], $SnO_2$ [5], $Ta_2O_5$, $TiO_2$ [6], $WO_3$ [7], etc. [8]. But the performance of some of these metal oxides appears to be average for pH sensing. Currently, the development of device having easy fabrication with low cast sensor membrane is the main focus in this area. Therefore, in this report, an effort was made in obtaining high pH sensitivity with low cost and easy fabrication of NiO nanostructure sensing membrane as a novel pH sensor based EGFET.

## 2 Experimental

### 2.1 Preparation of NiO Nanoflakes Sensing Membrane

The Nickel oxide (NiO) layers were deposited using chemical bath deposition (CBD) technique. All chemicals were of analytical reagent grade and used without further purification. De-ionized water was used in this synthesis and in washing steps of NiO layer deposition. The precursor solution for Nanoflakes Nickel oxide layer was obtained by dissolving 2.63 g (1 mol) of nickel sulphate hexahydrate ($NiSO_4.6H_2O$) in 10 ml and 2.24 g (1 mol) of potassium chloride (KCl) in 30 ml of deionized water. Further of it; 40 ml of 35% ammonia solution was added as complex agent. Colour changes were observed in the solution upon addition of ammonia, demonstrating the precipitation of nickel hydroxides particles from pale-green to blue-violet colour [9]. The complex agents used slow down the precipitation action and enables the formation of $Ni(OH)_2$ [10]. The total volume of the solution was made up to 100 ml by adding 20 ml of de-ionized water solution into 100 ml beaker. The mixture was maintained at 300 rpm stirring of approximately 30 min. The pH of the resultant

solution was measuring to be 13 due to excess ammonia solution. ITO/glass was used as the substrates in this study. The substrates layers were chemically and ultra-sonically cleaned before deposition, in acetone and ethanol for 900 s at 40 °C to elim-inating any greasy track then rinsed with de-ionized water. The clean substrates were immersed vertically in the solution and then heated. The deposition of Nanoflakes Nickel hydroxide was made at a solution temperature of 90 $^0$C. The sample was annealed at 300 °C temperature for 90 min.

## 2.2 Characterization Techniques

X-ray diffraction analyses were obtained with an X-ray diffraction high resolu-tion system (Model: Panalytical X'Pert PRO MRD PW3040) consisted of CuKα (1.5406 Å) radiation. The nanostructures and surface morphology of the films were analysed with a Field Emission Scanning Electron Microscopy (FESEM Model: FEI Nova NanoSEM 450).

## 2.3 Measurement of pH Sensor

The analysis of NiO nanoflakes membranes was made using two (2) different source meter (Keithley Series 2400) through personal computer (PC) system cable connec-tion. Measurement was carried out using LabTracer software that aids in initiating the pH sensor measurements by input data and receiving output data signal which were saved and analysis as well. The setup measurement for the pH sensor is shown in Fig. 1. The NiO nanoflakes sensing membrane was placed at the bottom of elec-trochemical cell that contains the pH buffer solution. The connection of the cell was made through the gate terminal of a commercially standard MOSFET (CD4007UB). Ag/AgCl electrode was employed as the reference electrode due to its provision of stable reference voltage to the sensing system [11]. The reference electrode was inserted into the pH buffer solution contained inside the cell. The measurement was carried out at room temperature (RT) (25 $^{°C}$) and wait for 60 s before the begin-ning of the pH measurements. The reference electrode was connected to the one of the source meter for inputting reference voltage ($V_{REF}$) to the electrode while the second source meter was used to input the drain-source voltage ($V_{DS}$) to the drain and source terminals of the MOSFET for drain-source current ($I_{DS}$) output readingand then measured the current–voltage (I–V) characteristics in pH = 4, 6, 8, 10 and 12 pH buffer solutions at RT. The $V_{DS}$ was set at 0.3 V, which is the voltage between the drain and the source of the MOSFET and the $V_{REF}$ was set at 3 V, which is the voltage that supply to the reference electrode.
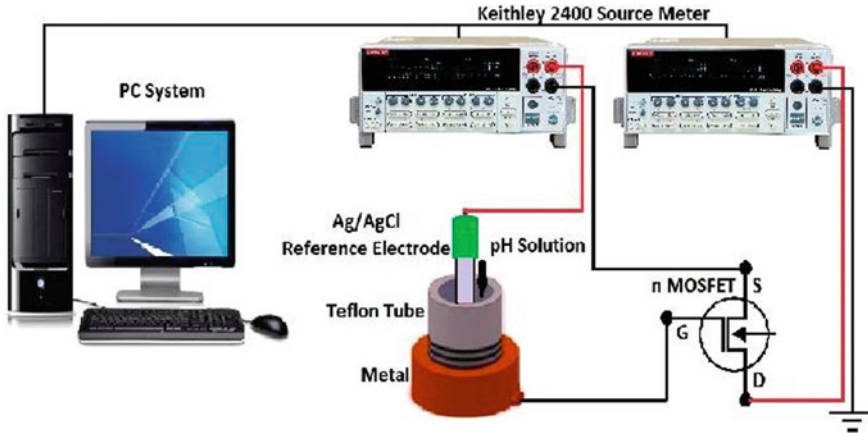
**Fig. 1** Setup diagram of pH sensor measurement system

## 3 Results and Discussion

Figure 2 shows the X-ray diffraction pattern and the values related to peaks of chemically grown, nanoporous Ni(OH)$_2$ with the subsequent annealed sample at 300 °C. From the pattern of the as-grown films sample, the Ni(OH)$_2$ phase was identified. The peaks at 33.15°, 38.62°, 59.18°, 62.73° and 72.68° that were labeled according to the (ICSD 00-014-0117) with Hexagonal unit cell parameters of a = 3.1260 (Å), b = 3.1260 (Å) and c = 4.6050 (Å) with angles Alpha = 90°, Beta = 90° and Gamma
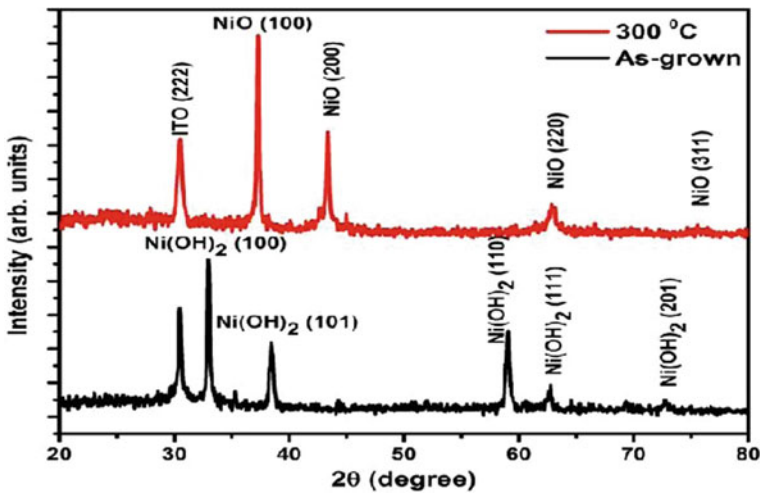


**Fig. 2** XRD pattern of the NiO/Ni(OH)$_2$ nanoflakes as-grown and at 300 °C

= 120°. Also, the peak for cubic ITO structure pattern has been identified for both as-grown and annealed sample with peak orientation of (222) at $2\theta = 30.62°$.

Meanwhile, X-ray diffraction annealed samples that attribute to cubic NiO was detected for the films on ITO/Glass substrate (00-047-1049) crystals with the lattice parameter of a, b and c = 4.1771 Å, and angle of $\alpha = \beta = \gamma = 90$. The peaks obtained were at $2\theta = 37.25°$, $43.28°$, and $62.88°$ with the preferential orientation of the films being at (100), (200) and (220) respectively, that indicates high crystallinity with the well defined intense peak at (100) indices. This indicates the formation of polycrystalline NiO films after annealing, with no trace of $Ni(OH)_2$ phase on the treated films. Which shows a complete $Ni(OH)_2$ to NiO transformation. The mean size of the crystallite (D) was estimated based on the full width at the half maximum (FWHM) peak position and the corresponding angle values was obtained, using Scherer's equation of Eq. (1). A small crystal size of 19.84 nm was obtained.

$$D = \frac{0.9\lambda}{\beta \cdot \cos\theta} \tag{1}$$

where: D is the mean size of the crystalline, K is a dimensionless shape factor, $\lambda$ is the X-ray wavelength; $\beta$ is the line broadening at half the maximum intensity (FWHM) in radian and $\theta$ is the Bragg angle.

FESEM measurements were carried out in order to determine the micro/nanostructural properties of the chemically deposited NiO films; as shown in Fig. 3. It can be seen that the $NiO/Ni(OH)_2$ films consists of grown porous net-like structure made up of interconnected nanoflakes' wall with a thickness of 30–70 nm of the annealed samples. The diameter of pores ranges from 50 to 300 nm with an observable difference on the dimension of thin films micro/nanostructure as the 300 °C, that shows high surface to volume ratio. The flakes wall appears to have a
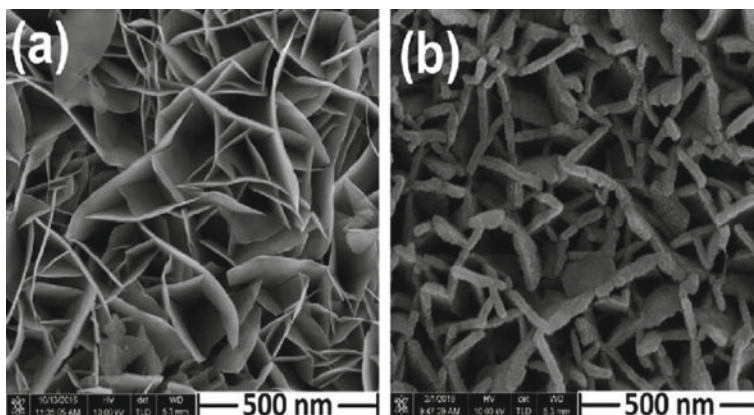


**Fig. 3** FESEM image and EDS spectrum nanoflakes for **a** as-grown $Ni(OH)_2$ and **b** 300 °C NiO annealed sample

**Table 1** Atomic and the weightpercent of the as-grown and annealed sample obtained from EDS EDX spectrum

| Sample | As grown | | 300 °C | |
|---|---|---|---|---|
| Element | O | Ni | O | Ni |
| Atomic % | 60.23 | 38.77 | 50.16 | 49.84 |
| Weight % | 29.51 | 70.49 | 21.35 | 78.65 |

rough surface with annealing temperature. The porous nanostructure, surface roughness and surface to volume ratio can be an important factor that provides easy access of ions surface reaction in sensor application [12] (Table 1).

The atomic ratio O: Ni of the 300 $^0$C sample appears with non-stoichiometric value, which makes it behave as a p-type material due Nickel vacancy.

### 3.1 Sensitivity and Linearity of pH Sensor

At the first contact of nanostructures NiO with an electrolyte, primary adsorption of [OH$^-$] and [H$^+$] occurs. This procedure is made at a low degree of the surface coverage. Furthermore, the surface reaction (NiO–OH) group occurs with [OH$^-$] ions in basic solution and [H$^+$] ions in acidic solution. The rate of this reaction is associated with the free electrons or holes concentration at the surface. The process involves charge transfer to the solid, which is distributed by transport of electron over the near surface region of the solid to create a depletion layer in solution of acid and then to improved or generate an accumulation layer at the base. The site-dissociation model was established to describe the oxide layer charging mechanism in the pH sensor [8]. The oxide charging as the result of equilibrium between the AOH and H$^+$ ions surface sites in the solution bulk was given. The surface reactions were as follows [13]

$$\text{AOH} \overset{K_A}{\leftrightarrow} \text{AO}^- + \text{H}_S^+ \tag{2}$$

$$\text{AOH}_2^+ \overset{K_B}{\leftrightarrow} \text{AOH} + \text{H}_S^+ \tag{3}$$

where H$_S^+$ is the H$^+$ ions located close to the solid surface and $K_A = \frac{[\text{AO}^-][\text{H}^+]_S}{[\text{AOH}]}$ and $K_B = \frac{[\text{AOH}][\text{H}^+]_S}{[\text{AOH}_2^+]}$ are the equilibrium constants of Eqs. (2) and (3) respectively AO$^-$, AOH$_2^+$ and AOH represent negative, positive and neutral surface sites, respectively. $[\text{AO}^-]$ $[\text{AOH}_2^+]$ and [AOH] are the numbers of these sites per surface area. $[\text{H}^+]_S$ is the H$^+$ ions surface activity.

In view of the pH electrode, the surface potential is obtained by the H$^+$ ions exchange between the binding sites on the surface of the sensing membrane and the

solution. Also, the pH electrode selectivity and chemical sensitivity are controlled by the properties of electrolyte/insulator interface. The pH electrode response obeys the Nernstian equation, which represent straight line equation as;

$$E = E_O - \frac{RT}{nF} In([H^+]) \tag{4}$$

$$E = E_O + Slope(T) \cdot \text{pH} \tag{5}$$

where $E$ is the measured potential, $E_0$ is a characteristic constant for the ion-sensitive/external electrode system, and the slope factor term "$RT/F$" is known as the Nernst factor, which provides the amount of change in total potential (mV) for all change in pH unit. $T$ the absolute temperature (in Kelvin), n is the signed ionic charge, R is the gas constant, $F$ the Faraday constant and [H$^+$] the molar concentration of the free ionic species. Nernst equation describes electrochemical cell potential as a function of ions concentrations taking part in the reaction. The ideal response was assumed to be 59.2 mV/pH at 25 °C [14].

Based on the site binding theory, the number of binding sites residing on the sensing membrane could result to changes in the surface potential voltage between the electrolyte and the interface of the sensing layer which depend on pH at point of zero charge (pH$_{pzc}$). The actual change in surface potential voltage would depend on the pH value of the electrolytic solution. Based on the above mentioned site binding model, the surface potential voltage of NiO films between the electrolytic pH solution interface and the sensing layer can be expressed as [15];

$$\psi = 2.303 \frac{kT}{q} \frac{\beta}{\beta + 1} (\text{pH}_{pzc} - \text{pH}) \tag{6}$$

where, $\beta = \frac{2q^2 N_S \left(\frac{K_B}{K_A}\right)^{1/2}}{kT C_{DL}}$ is the sensitivity parameter, which is dependent on the surface density of hydroxyl groups and reflects the chemical sensitivity of the gate insulator, $\text{pH}_{pzc} = -\log_{10}\left(\frac{K_A}{K_B}\right)^{1/2}$ is the pH value at the zero charge point of the sensing membrane, K$_A$ and K$_B$ are acid and base equilibrium constants, respectively. $N_S$ is the total number of surface sites per unit area, $C_{DL}$ is the electrical double layer capacitance derived by the Gouy–Chapman–Stern model, $k$ is Boltzmann's constant, $T$ is the absolute temperature, $q$ is the charge of an electron [3].

Similar to the MOSFET, the linear relationship between the gate voltage ($V_G$) and the drain current ($I_D$) for an EGFET is expressed as [16];

$$I_D = \mu_n C_{ox} \frac{W}{2L} \left[2V_{DS}(V_{GS} - V_{TH}) - V_{DS}^2\right] \tag{7}$$

where $L$ is the gate length, $\mu_n$ is the charge-carrier effective mobility, $C_{ox}$ is the gate oxide capacitance per unit area and $W$ is the gate width, $V_{DS}$ is the drain-source voltage and $V_{TH}$ is the threshold voltage of MOSFET relating to the surface

potential[17]. Base on this sensing model, the pH sensitivity is therefore defined as [18]:

$$Sensitivity = \frac{\Delta \psi}{\Delta \text{pH}} = \frac{\Delta V_{TH}}{\Delta \text{pH}} = \frac{\Delta V_{GS}}{\Delta \text{pH}} \tag{8}$$

In the acidic region, more positive surface potential of the NiO films leads to a smaller applied gate voltage. As the pH value raises, the $V_G$ value increased as well. Accordingly, the pH sensitivity measurement can be obtained from the slope of gate voltage $V_G$ versus pH solution.

The commercial MOSFET (CD 4007UB) has been confirmed to be a eligible EGFET transducer due to its good linearity of over 99%. For operation of EGFET at $V_{GS} = 3$ V, it is within the operational region in pH values conversion to $I_{DS}$ with remarkable sensitivity. The MOSFET controls the electron-holes flow from source (S) to drain (D) by the control of size and shape of the conductive channel. The channel size controls the gate-source voltage (Vgs) positivity ([H$^+$]) or negativity ([OH$^-$])). The $I_{DS}$ dependency on the pH value is because of the accumulation of [H$^+$] ions in the acidic solution on the sensing surface, which is similar to applying an additional positive voltage at the MOSFET gate [14]. This would result to increase of the conductive channel with increase of the concomitant current. On the contrary, the conductive channel constricted or closed for the basic solution with extra negative voltage application, hence, current decreases as shown in Fig. 4 [17].

Figure 4 shows the (I–V) characteristics for NiO membranes using the Fig. 1 setup with different pH value of 4, 6, 8, 10 and 12 buffer solutions. Figure 4a, b indicates the ($I_{DS}$–$V_{GS}$) and ($I_{DS}$–$V_{DS}$) curves for linear regimes and saturation, respectively. In the saturation regime, $V_{GS}$ was set fixed at 3 V, and in linear regime, $V_{DS}$ was set fixed at 0.3 V. The (I–V) curves were then plotted to get the sensitivity for both membranes from the slope of Fig. 4c, d.

The current was decrease with the increase in pH value in the saturation regime while the threshold voltage shifted to the right with increase in the pH value. In the saturation regime, where the low pH value is similar to high accumulation of H$^+$ ions in the acidic solution on the sensing surface. The high amounts of ions result in additional positive voltage to be applied to the gate, in which conductive channel increases but depletion region decreases, hence current increases. Unlike for a basic solution, where the high pH value denoting high OH$^-$ ions and low H$^+$ ions is equivalent to applying negative voltage to the gate, the conductive channel decreases through increasing the depletion region, thereby decreasing the current flow. Such voltage is inversely proportional to the current, the threshold voltage shifted to the right with the increase in the pH value for the linear regime. As a result, voltage is directly proportional to pH value.

The site-binding model was used in this research work to show the chemical processes that take place at the interface between the available [H$^+$] ions in the electrolyte and membrane. The membrane material elements enclose water shells, which hinders any contact with the interface and inhibit chemical reactions, thus the small sized [H$^+$] ions will neither be hydrated nor shelled. This feature facilitates
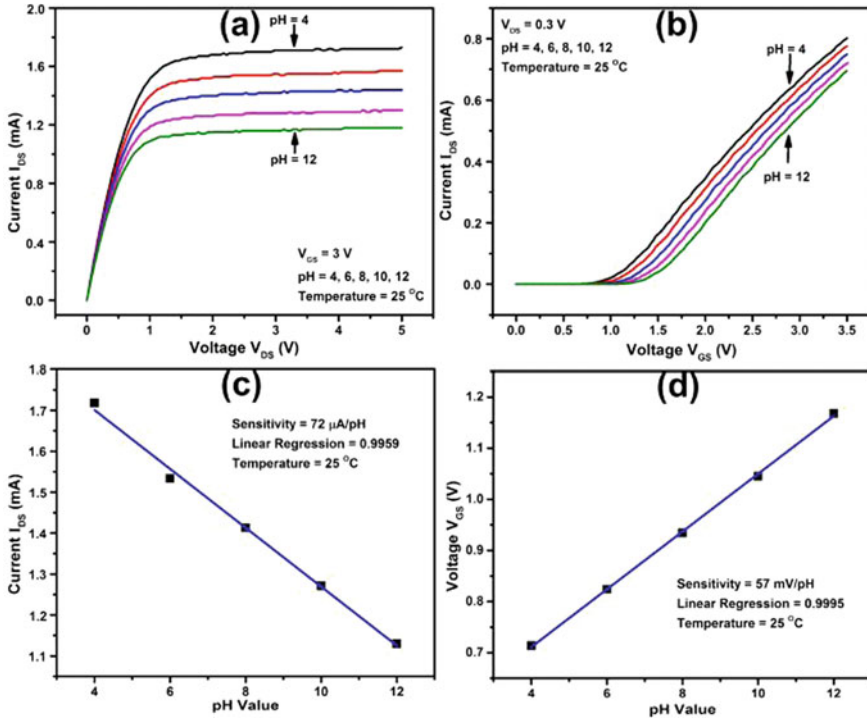
**Fig. 4** I-V curve characteristics in **a** saturation and **b** linear regime with corresponding sensitivity and linearity **c** and **d** NiO membrane

chemical reactions at the interface. On the contrary, $[OH^-]$ ions are the only ions that can bond to the available sites on the interface surface.

Linearity and Sensitivity can be determined by linear fitting between $I_{DS}$ and $V_{GS}$ values against pH values obtained at fixed value of $V_{DS}$ (4 V) and fixed value of $I_{DS}$ (0.4 mA) of the I-V curves of Fig. 4 respectively using Eq. (8). From the linear fitting, the voltage sensitivity obtained as slope and linearity as linear regression of NiO membrane were found to be 57 mV/pH; 0.9995 and 72 μA/pH; 0.9959, for both linear ($I_{DS}-V_{GS}$ characteristics) and saturation ($I_{DS}-V_{DS}$ characteristics) regimes, respectively as shown in Fig. 4d, c. The result obtained is much better than the earlier report works using NiO as membrane for pH sensing [17, 19]. This apparent improvement in sensitivity can be associated to the high surface-to-volume ratio with the small sized NiO nanoporous crystals and its high crystallinity, which provides more surface binding sites and larger effective sensing areas. The NiO nanostructures have a larger surface area for adsorbing additional $OH^-$ and $H^+$ ions and have increased oxygen-related binding that could sense H + ions effectively in the acid solution region. The result suggests that the Nanoflakes NiO membrane synthesis based on Chemical Bath Deposition is potentially an essential materials for EGFET based pH sensors.

## 4    Conclusion

Nanoflakes NiO membrane was made using Chemical Bath Deposition to determine its applicability as EGFET based pH sensors. The structural and morphological characteristics of the membranes were analyzed using FESEM and XRD. The NiO membrane sensitivity (57 mV/pH) was found to be relatively higher than the works reported previewly on NiO membrane as pH sensor, due to the high crystallinity, small crystal size and high porosity properties of NiO Nanostructured layer, which provided higher number of sites with surface area and increased the number of exchangeable ions with the [H$^+$] that exist in the electrolyte.

## References

1. Sabah, F.A., Ahmed, N.M., Hassan, Z., Al-Hardan, N.H.: Sensitivity of CuS and CuS/ITO EGFETs implemented as pH sensors. Appl. Phys. A Mater. Sci. Process. **122**(9), 1–6 (2016)
2. Yossawat, R., et al.: High sensitive nanocrystal titanium nitride EG-FET pH sensor. Adv. Mater. Res. **802**(September), 232–236 (2013)
3. Tsai, C., Chou, J., Sun, T., Hsiung, S.: Study on the sensing characteristics and hysteresis effect of the tin oxide pH electrode. Sens. Actuators B Chem. **108**, 877–882 (2005)
4. Chang, S., et al.: Investigation of ZnO-nanowire-based extended-gate field-effect-transistor pH sensors prepared on glass substrate. Sci. Adv. Mater. **4**(xx), 1–5 (2012)
5. Fernandes, J.C., Nascimento, R.A.S., Mulato, M.: Effects of measurements conditions on an extended-gate FET used as pH sensor. Mater. Res. **19** (2016)
6. Rosdan, M.A., Herman, S.H., Abdullah, W.F.H., Kamarozaman, N.S., Syono, M.I.: Sputtered titanium dioxide thin film for extended-gate FET sensor application, pp. 219–222 (2013)
7. De Castro, R., Tadeu, D., Mulato, M., Maria, E.: Comparative sensibility study of WO 3 ph sensor using EGFET and ciclic voltammetry. Mater. Res. **18**(1), 15–19 (2015)
8. Wu, S., Wu, Y., Lin, C.: High performance ISFET-based pH sensor utilizing low-cost industrial-grade touch panel film as the gate structure, pp. 2131–2133 (2014)
9. Adekunle, A.S., et al.: Comparative catalytic properties of Ni(OH)$_2$ and NiO nanoparticles towards the degradation of nitrite (NO$_2$\n-) and nitric oxide (NO). Int. J. Electrochem. Sci. **9**(6), 3008–3021 (2014)
10. Ezema, F.I., Ekwealor, A.B.C., Osuji, R.U.: Optical properties of chemical bath deposited CdS thin films. J. Optoelectron. Adv. Mater. **9**(6), 1898–1903 (2007)
11. Khanna, V.K.K.V.: Fabrication of ISFET microsensor by diffusion-based Al gate NMOS process and determination of its pH sensitivity from transfer characteristics. Indian J. Pure Appl. Phys. **50**(3), 199–207 (2012)
12. Inamdar, A.I., Kim, Y., Pawar, S.M., Kim, J.H., Im, H., Kim, H.: Chemically grown, porous, nickel oxide thin-film for electrochemical supercapacitors. J. Power Sources **196**(4), 2393–2397 (2011)
13. Ali, G.M., Dhaher, R.H., Abdullateef, A.A.: pH sensing characteristics of EGFET based on Pd- Doped ZnO thin films synthesized by sol-gel method. **4**(2), 234–238 (2015)

14. Wu, Y.-L., Chang, S.-P., Chang, S.-J., Weng, W.Y., Lin, Y.-H.: A novel ph sensor using extended-gate field-effect transistors with $Ga_2O_3$ nanowires fabricated on a novel pH sensor using extended-gate. Sci. Adv. Mater. **6**, 1–4 (2014)
15. Chiu, Y., Tseng, C., Lee, C.: Nanostructured EGFET pH sensors with surface-passivated ZnO thin-film and nanorod array. IEEE Sens. J. **12**(5), 930–934 (2012)
16. Huang, B., Lin, J., Yang, Y.: ZnO/silicon nanowire hybrids extended-gate field-effect. **160**(6), 78–82 (2013)
17. Lin, F., Chang, H., Hsiao, S.: Preparation and characterization of nickel oxide-based EGFET pH sensors. In: Ninth International Conference on Sensing Technology Preparation, pp. 402–405 (2015)
18. Vieira, N.C.S., Figueiredo, A., Faceto, A.D., De Queiroz, A.A.A., Zucolotto, V., Guimarães, F.E.G.: Sensors and actuators B: chemical dendrimers/$TiO_2$ nanoparticles layer-by-layer films as extended gate FET for pH detection. Sens. Actuators B. Chem. **169**, 397–400 (2012)
19. Ibupoto, Z.H., Khun, K., Willander, M.: Development of a pH sensor using nanoporous nanostructures of NiO. J. Nanosci. Nanotechnol. **14**(9), 6699–6703 (2014)